

# Bidirectional thermotaxis in *Caenorhabditis elegans* is mediated by distinct sensorimotor strategies driven by the AFD thermosensory neurons

Linjiao Luo<sup>a,b,1,2</sup>, Nathan Cook<sup>c,3</sup>, Vivek Venkatachalam<sup>b,3</sup>, Luis A. Martinez-Velazquez<sup>c,3</sup>, Xiaodong Zhang<sup>d,3</sup>, Ana C. Calvo<sup>c</sup>, Josh Hawk<sup>c</sup>, Bronwyn L. MacInnis<sup>e</sup>, Michelle Frank<sup>b</sup>, Jia Hong Ray Ng<sup>b</sup>, Mason Klein<sup>b</sup>, Marc Gershow<sup>b</sup>, Marc Hammarlund<sup>c</sup>, Miriam B. Goodman<sup>e,1,2</sup>, Daniel A. Colón-Ramos<sup>c,1,2</sup>, Yun Zhang<sup>d,1,2</sup>, and Aravinthan D. T. Samuel<sup>b,1,2</sup>

<sup>a</sup>Key Laboratory of Modern Acoustics, Ministry of Education, Department of Physics, Nanjing University, Nanjing 210093, China; <sup>b</sup>Department of Physics and Center for Brain Science, Harvard University, Cambridge, MA 02138; <sup>c</sup>Program in Cellular Neuroscience, Neurodegeneration, and Repair, Department of Cell Biology, Yale University School of Medicine, New Haven, CT 06536; <sup>d</sup>Department of Organismic and Evolutionary Biology and Center for Brain Science, Harvard University, Cambridge, MA 02138; and <sup>e</sup>Department of Molecular and Cellular Physiology, Stanford University School of Medicine, Stanford, CA 94305

Edited\* by Paul W. Sternberg, California Institute of Technology, Pasadena, CA, and approved January 8, 2014 (received for review August 13, 2013)

The nematode *Caenorhabditis elegans* navigates toward a preferred temperature setpoint ( $T_s$ ) determined by long-term temperature exposure. During thermotaxis, the worm migrates down temperature gradients at temperatures above  $T_s$  (negative thermotaxis) and performs isothermal tracking near  $T_s$ . Under some conditions, the worm migrates up temperature gradients below  $T_s$  (positive thermotaxis). Here, we analyze positive and negative thermotaxis toward  $T_s$  to study the role of specific neurons that have been proposed to be involved in thermotaxis using genetic ablation, behavioral tracking, and calcium imaging. We find differences in the strategies for positive and negative thermotaxis. Negative thermotaxis is achieved through biasing the frequency of reorientation maneuvers (turns and reversal turns) and biasing the direction of reorientation maneuvers toward colder temperatures. Positive thermotaxis, in contrast, biases only the direction of reorientation maneuvers toward warmer temperatures. We find that the AFD thermosensory neuron drives both positive and negative thermotaxis. The AIY interneuron, which is postsynaptic to AFD, may mediate the switch from negative to positive thermotaxis below  $T_s$ . We propose that multiple thermotactic behaviors, each defined by a distinct set of sensorimotor transformations, emanate from the AFD thermosensory neurons. AFD learns and stores the memory of preferred temperatures, detects temperature gradients, and drives the appropriate thermotactic behavior in each temperature regime by the flexible use of downstream circuits.

Navigational behaviors provide a framework for exploring the interplay among sensorimotor circuits, learning, and memory. During a navigational task, animals eventually reach their goals by implementing strategies composed of sensorimotor rules. Experience can modify navigational goals, so memory can also be integrated into sensorimotor pathways. Studying navigation in the nematode *Caenorhabditis elegans* offers the possibility of understanding the plasticity and programming of sensorimotor circuits from input to output in a small nervous system (1).

Previous studies established *C. elegans* thermotaxis as a model for experience-dependent navigation (2–6). When worms are exposed to specific temperatures between 15 °C and 25 °C for at least 4 h, they adopt those temperatures as their thermotactic setpoint ( $T_s$ ) (2, 3, 5, 7). When placed on a spatial temperature gradient, worms seek the  $T_s$ . When arriving near  $T_s$ , worms track isotherms. Genetic analysis of thermotaxis has yielded mutants that are athermotactic (crawling randomly on temperature gradients), cryophilic (crawling to the coldest point on a temperature gradient irrespective of  $T_s$ ), or thermophilic (crawling to the warmest point on a temperature gradient). This observation led to the suggestion that thermotaxis might

involve separate circuits for negative thermotaxis (movement down gradients) and positive thermotaxis (movement up gradients) that balance near  $T_s$  (2, 4).

Systematic laser ablation analysis uncovered an interconnected neural circuit for thermotaxis behavior composed of one pair of thermosensory neurons (AFD) and three pairs of interneurons (AIY, AIZ, and RIA) (Fig. 1A) (4). Ablation of AFD or AIY led to cryophilic behavior. Ablation of AIZ led to thermophilic behavior. Ablation of RIA led to athermotactic behavior. Ablation of the AWC olfactory neuron, which is presynaptic to AIY and RIA, has also been found to mildly disrupt negative thermotaxis (8). These findings suggested that candidate circuit pathways converging on RIA might drive positive and negative thermotaxis (Fig. 1A).

Recently, movie microscopy has enabled high-resolution and high-content tracking of worm navigation (5, 9–12). Tracking negative thermotaxis and isothermal tracking have uncovered

## Significance

The nematode *Caenorhabditis elegans* offers the opportunity to map complex behaviors to the specific roles of each neuron in a 302-neuron nervous system. Thermotaxis is a complex behavior where the worm inverts the behavioral mode—positive thermotaxis up gradients or negative thermotaxis down gradients—to move toward a remembered temperature. How are both long-term memory and multiple behavioral modes encoded? A long-standing model has been that separate circuits for positive and negative thermotaxis compete for control of body movement. In contrast, we find that different modes of thermotaxis are driven by one set of AFD thermosensory neurons. Circuits for different thermotactic behaviors diverge from the AFD neurons, probably by coupling sensory inputs to motor programs in different ways to create different thermotactic behaviors.

Author contributions: L.L., V.V., M.B.G., D.A.C.-R., Y.Z., and A.D.T.S. designed research; L.L., N.C., V.V., L.A.M.-V., A.C.C., J.H., B.L.M., M.F., and J.H.R.N. performed research; L.L., V.V., X.Z., A.C.C., J.H., B.L.M., M.K., M.G., and M.H. contributed new reagents/analytic tools; L.L. and V.V. analyzed data; and L.L., M.B.G., D.A.C.-R., Y.Z., and A.D.T.S. wrote the paper.

The authors declare no conflict of interest.

\*This Direct Submission article had a prearranged editor.

<sup>1</sup>L.L., M.B.G., D.A.C.-R., Y.Z., and A.D.T.S. contributed equally to this work.

<sup>2</sup>To whom correspondence may be addressed. E-mail: samuel@physics.harvard.edu, lluo@fas.harvard.edu, mbgoodman@stanford.edu, daniel.colon-ramos@yale.edu, or yzhang@oeb.harvard.edu.

<sup>3</sup>N.C., V.V., L.A.M.-V., and X.Z. contributed equally to this work.

This article contains supporting information online at [www.pnas.org/lookup/suppl/doi:10.1073/pnas.1315205111/-DCSupplemental](http://www.pnas.org/lookup/suppl/doi:10.1073/pnas.1315205111/-DCSupplemental).

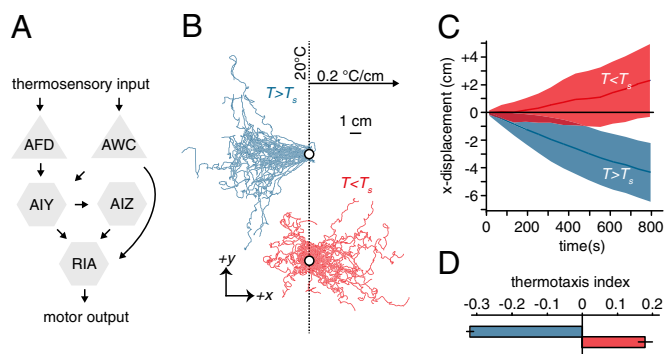


**Fig. 1.** Bidirectional thermotaxis in *C. elegans*. (A) A proposed neural circuit for thermotaxis showing chemical synaptic connectivity between the AFD and AWC sensory neurons and downstream interneurons. (B) Navigation trajectories over 15 min of 50 wild-type (N2) worms grown at 15 °C (blue) or 25 °C (red) and started near 20 °C on a 0.2 °C/cm linear spatial temperature gradient on a 22- × 22-cm agar plate (Fig. S1). Trajectories are aligned to the same starting point (white circle) for presentation purposes. (C) Mean x displacement  $\pm$  1 SD for trajectories shown in B. (D) A navigational index was computed for each trajectory using the component of velocity in the direction of the gradient divided by the mean crawling speed along each trajectory. Positive and negative thermotaxis corresponds to positive and negative indices, respectively. The magnitude of the index for negative thermotaxis is significantly larger than that for positive thermotaxis ( $P < 0.0005$  using Student *t* test). All data points in C and D represent mean  $\pm$  1 SEM. Each calculation is based on at least 241 worm trajectories.

components of the worms' underlying behavioral strategies (12–14). Negative thermotaxis involves modulation of run length that is reminiscent of the biased random walk that was originally observed in bacterial chemotaxis (15, 16). In isotropic environments, worms move in a sequence of forward movements (runs) interrupted by turns and reversal turns (also called pirouettes) generating exploration that resembles an unbiased random walk. During negative thermotaxis, if worms sense negative temperature gradients, they suppress turns and reversal turns, yielding long runs in the favorable cooler direction. If worms sense positive temperature gradients, they exhibit short runs. Thus, net migration is down temperature gradients (13). Isothermal tracking is deterministic, a steering behavior in which the worm continuously makes temperature comparisons and movement corrections with every undulation to maintain isothermal alignment (14).

The strategy for positive thermotaxis has not yet been analyzed because this behavior is restricted to certain growth and stimulus conditions. If worms are grown at  $\sim 23$  °C or higher, they will crawl up temperature gradients toward their  $T_s$  as long as they are within  $\sim 5$  °C and navigating gradients are shallower than 0.5 °C/cm. Lower setpoints, steeper gradients, and greater distances from the  $T_s$  lead to athermotactic behavior (17). Now that we know specific conditions that evoke positive thermotaxis, we can use these conditions to compare and contrast the strategies for positive and negative thermotaxis.

Genetic methods provide tools to inactivate or remove specific neurons from *C. elegans* that yield larger numbers of animals than is possible with laser ablation. Cell-specific expression of reconstituted caspase (recCaspase) induces programmed cell death and thus the removal of specific neurons during development (18). Expression and irradiation of the protein KillerRed with intense green light remove cells acutely (19, 20). Here, we combine these methods with quantitative behavioral tracking to assess how each neuron in the proposed circuit for thermotaxis (AFD-AWC-AIY-AIZ-RIA) contributes to movement up or down temperature gradients.

We find that positive thermotaxis involves biased reorientation toward the  $T_s$ ; the worm uses turns and reversal turns to point itself toward warmer temperatures. We find that negative thermotaxis also involves biased reorientation toward the  $T_s$ ; the

worm uses turns and reversal turns to point itself toward colder temperatures. As observed earlier, negative thermotaxis also involves a biased random walk toward the  $T_s$ , with longer runs toward colder temperatures and shorter runs toward warmer temperatures. These results suggest an asymmetry in the sensorimotor strategies for positive and negative thermotaxis, where run-length modulation makes negative thermotaxis more efficient by prolonging favorable orientations. We find that AFD drives both positive and negative thermotaxis. AIY is necessary to exhibit positive instead of negative thermotaxis below  $T_s$ . Although AWC, AIZ, and RIA might have minor contributions to thermotaxis, none of these neurons is required for either positive or negative thermotaxis. In summary, bidirectional thermotaxis emanates from the AFD neurons, achieved by coupling sensory input to motor output in different patterns to drive thermotaxis up gradients below  $T_s$  and down gradients above  $T_s$ .

## Results

**Strategies for Negative and Positive Thermotaxis Behaviors.** We used high-pixel density movie cameras to record the movements of individual young adult worms performing thermotaxis across the surfaces of 22- × 22-cm agar plates with a shallow linear spatial temperature gradient (0.2 °C/cm) centered near 20 °C. With this gradient steepness and starting temperature, worms grown at 25 °C will move toward the warm side of the plate and worms grown at 15 °C will move toward the cold side of the plate, pursuing  $T_s$  in either direction (Fig. 1 B and C) (17). Large space for thermotaxis allowed us to study many worms at once. High-pixel density cameras allowed us to segment trajectories based on worm posture, even at low magnification, into a sequence of periods of forward movement, backward movement, and sharp turns. In this setup, many uninterrupted thermotaxis trajectories of individual worms can be obtained in each experiment, increasing the quality of statistical analysis.

An index of thermotaxis efficiency is provided by the ratio between the mean velocity in the gradient direction of each trajectory and crawling speed:  $\langle v_x \rangle / \langle v \rangle$  (Fig. 1D). This index is +1 if the worm strictly moves straight up the gradient and  $-1$  if it strictly moves straight down the gradient. We found that negative thermotaxis is more efficient than positive thermotaxis. To better understand this, we turned to detailed analysis of individual animal movements. Net movement up or down gradients is the product of sensorimotor rules enacted along the navigational trajectory. We sought to extract these rules for positive and negative thermotaxis.

In isotropic environments, crawling locomotion is an alternating sequence of periods of forward movement (runs) and reorientation maneuvers. Reorientation maneuvers are either turns or reversal turns (also called pirouettes) (12, 13, 15) (Fig. 2 A and B and Movie S1). First, we examined the statistics of run duration, the time intervals between successive reorientation maneuvers. As before for negative thermotaxis, we found that worms exhibited longer runs when headed down gradients than up gradients (11–13, 21) (Fig. 2C). During positive thermotaxis, run durations were roughly the same whether up or down gradients (Fig. 2C).

Next, we examined the possibility of steering to select favorable directions either during runs or by reorientation maneuvers. Steering mechanisms (also called weathervaning) have been identified in *C. elegans* chemotaxis (11, 21, 22). To look for steering mechanisms, we focused on runs pointed orthogonally to the gradient. If the worm was capable of steering during a run, the run should gradually veer toward preferred directions. However, we found that runs veered toward the preferred and nonpreferred directions by similar amounts during either negative or positive thermotaxis (Fig. 2D). If the worm used reorientation maneuvers to pick the direction of new runs after runs pointed orthogonally to the gradient, it should be able to bias new runs to be up the gradient during positive thermotaxis or down the gradient during negative thermotaxis. For both positive

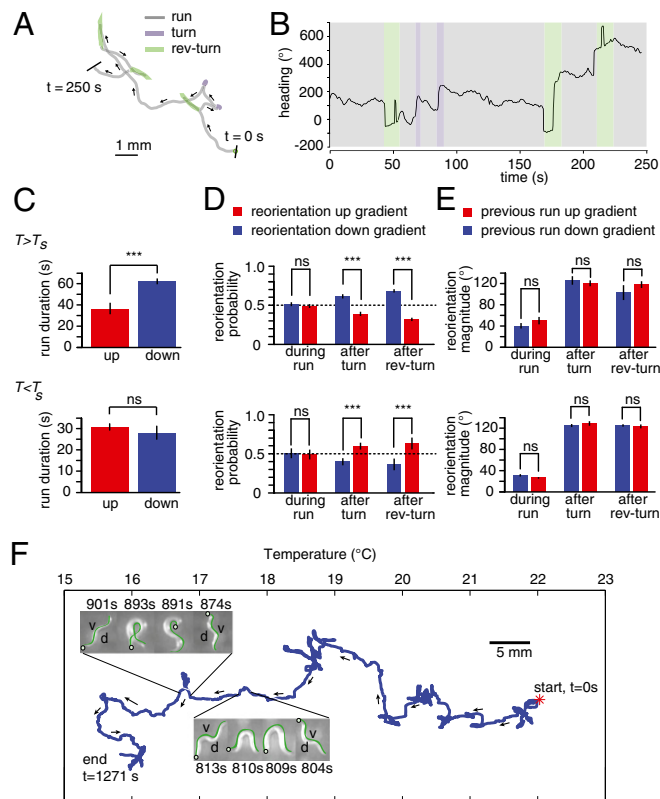


**Fig. 2.** Strategies for bidirectional thermotaxis. (A) Representative 250-s trajectory of a crawling worm segmented using machine-vision software that detects forward movements (gray), turns (purple), and reversal turns (green) on the basis of posture and movement (*Materials and Methods* and *Movie S1*). (B) Orientation with respect to the gradient is continuously monitored for each worm during thermotaxis (data for trajectory in A is represented), and the frequency, direction, and size of reorientation maneuvers are calculated to assess navigational strategy. For presentation purposes, the orientation angle is unwrapped so that continuous changes in heading that pass through  $0^\circ$  do not cause  $360^\circ$  jumps. (C) During negative thermotaxis (*Upper*), runs down the temperature gradient (blue) are longer than runs up the gradient (red). During positive thermotaxis (*Lower*), runs up and down the gradient are in the same duration. Calculations are based on runs with orientations within  $45^\circ$  of the gradient axis. (D) During negative thermotaxis (*Upper*) or positive thermotaxis (*Lower*), runs orthogonal to the gradient veer toward warmer temperatures and colder temperatures with equal likelihood. After runs orthogonal to the gradient, the worm uses reorientation maneuvers to bias new runs toward preferred temperatures. (E) During negative (*Upper*) or positive thermotaxis (*Lower*), the size of angular reorientation between the beginning and end of runs down the gradient are the same as for runs up the gradient. The size of angular reorientation after turns or reversal turns that terminate runs down the gradient are the same size as those for runs up the gradient. All data points in C–E represent mean  $\pm$  1 SEM. Calculations are based on runs with orientations within  $45^\circ$  of the gradient axis taken from 241 to 309 worm trajectories.  $***P < 0.0005$  using Student *t* test. ns, no significant difference. (F) A representative center-of-mass trajectory of an individual wild-type young adult worm grown at  $15^\circ\text{C}$  and started at  $22^\circ\text{C}$  on a linear temperature gradient is shown. Movements on a spatial gradient were tracked on a compound microscope (*Materials and Methods*). During negative thermotaxis, the animal uses turns and reversal turns to orient itself toward colder temperatures. For this animal viewed from above, reorientation maneuvers that produced clockwise or counterclockwise heading changes involved ventral or dorsal bending, respectively. Portions of the trajectory are highlighted that involve a turn with dorsal bending (804–813 s) and a reversal turn with ventral bending (874–901 s). In each frame, the head is labeled with a circle and the ventral side is labeled with a green line. Similar trajectories were observed in a total of 10 individual worms.

and negative thermotaxis, we found that both turns and reversal turns were more likely to point new runs toward the  $T_s$  (Fig. 2D).

We also examined the size of heading changes, both by gradual reorientation during runs and by reorientation maneuvers. A plausible navigation mechanism is to make small heading changes when already headed in favorable directions, but larger heading changes when headed in unfavorable directions. This strategy is exhibited by *Drosophila* larva during thermotaxis (4, 22). However, we found no evidence that the size of heading changes was affected by initial orientation during thermotaxis (Fig. 2E).

Crawling worms lie on their left or right side, and thus steering to orient the animal toward preferred temperatures must involve bending toward the dorsal or ventral side. A high-resolution analysis of salt chemotaxis—carried out by monitoring the bending movements of worms subjected to chemical currents while held in microfluidic devices—has shown that worms can bend both dorsally and ventrally toward attractants (23). The large-format assay that we used to quantify thermotactic strategies (Fig. 2) lacks resolution to label the dorsal and ventral sides of each crawling animal. To look more closely at steering, we made a single-animal tracking system by placing a spatial temperature gradient on the motorized stage of a compound microscope. We found that reorientation maneuvers using both dorsal and ventral bending movements appeared along thermotactic trajectories (Fig. 2F).

Taken together, our results suggest that negative thermotaxis involves two strategies. During negative thermotaxis, the worm extends runs toward colder temperatures and shortens runs toward warmer temperatures and uses reorientation maneuvers to increase the likelihood that new runs are pointed toward colder temperatures. During positive thermotaxis in our setup, the worm relies on reorientation maneuvers to point runs toward warmer temperatures.

#### AFD Thermosensory Neuron Drives Both Positive and Negative Thermotaxis.

The principal thermosensory neurons in *C. elegans* are the AFD neurons, a bilateral pair that send sensory dendrites toward the amphid pore near the anterior tip of the worm. AFD was discovered to be involved in thermotaxis through laser ablation analysis. Killing AFD caused worms to either move to the coldest part of a temperature gradient (a cryophilic phenotype) or not to exhibit a thermal preference at all (an athermotactic phenotype). Killing AFD also abolished isothermal tracking behavior (4, 24).

A more recent laser ablation analysis of AFD quantified turn frequency, a measure of the biased random walk during negative thermotaxis. Swimming worms were exposed to warming or cooling temporal ramps at temperatures above or below the  $T_s$  (12, 24). Killing AFD disrupted the temperature-dependent modulation of turn frequency when worms should exhibit negative thermotaxis above  $T_s$ . Killing AFD did not create any turn frequency bias at temperatures below the  $T_s$ . The analysis of turn frequency in swimming worms subjected to temporal ramps would be sensitive only to the modulation of run duration, and the absence of a biased random walk component in positive thermotaxis (see above) may explain why the swimming assay has revealed only negative thermotaxis (12, 24). Because our experimental conditions allow us to examine and compare both positive and negative thermotaxis, we investigated the role of AFD in driving thermotaxis both above and below the  $T_s$ .

First, we used a genetic method to remove AFD by selectively expressing recCaspase (18). Coexpression of two subunits of the *C. elegans* CED-3 Caspase under the control of the AFD-specific promoter *gcy-8* leads to AFD cell death. We found that killing AFD diminished both positive and negative thermotaxis, suggesting that AFD regulates both behaviors (Fig. 3A). We also used an independent method of cell ablation with KillerRed, a photosensitive protein that kills cells upon green light illumination (25). We used transgenic lines that selectively expressed KillerRed in the AFD neurons and compared irradiated and nonirradiated animals 1 d after exposure. We verified destruction of the AFD neurons in the irradiated animals using

fluorescence microscopy. Consistent with recCaspase-mediated AFD ablation, we found that movements up and down thermal gradients were disrupted by KillerRed-mediated AFD ablation (Fig. 3A). We also examined a mutant, *ttx-1(p767)*, with a developmental defect in AFD owing to a mutation in the *Otx/otd* homolog *ttx-1* gene. Previously, it was shown that mutations in *ttx-1* diminished negative thermotaxis above the  $T_s$  and produced weak negative thermotaxis below the  $T_s$  (26). In our experimental setup, we found that *ttx-1*-mediated disruption of AFD development weakened negative thermotaxis above  $T_s$  and abolished positive thermotaxis below  $T_s$  (Fig. 3A). We note that the *ttx-1(p767)* allele disrupts AFD development without completely removing the neuron (26), which may explain the difference caused by partial loss of thermotactic movement by *ttx-1* mutation and complete loss by ablation.

**Analysis of Other Neurons in the Proposed Neural Circuit for Thermotaxis.** In the classic model for the thermotaxis neural circuit, competing circuits for positive and negative thermotaxis are integrated by downstream interneurons (4, 27). In particular, AIY and AIZ were proposed to drive positive and negative thermotaxis, respectively; RIA was proposed to integrate both pathways (Fig. 1A) (28). Next, we examined the contributions of these interneurons to positive and negative thermotaxis using our experimental setup.

We examined AIY using three different methods of cell disruption, the *ttx-3(ks5)* mutant that disrupts AIY development, and transgenic lines that specifically expressed recCaspase or KillerRed to remove AIY. In all three cases, we found that these worms moved down temperature gradients instead of moving up gradients when started at temperatures below the  $T_s$  (Fig. 3B). Laser ablation of AIZ has been reported to cause a thermophilic phenotype: worms lacking AIZ crawled to the warmest point on a spatial temperature gradient (4). Cell-specific promoters are not available for AIZ, and so we used laser ablation to remove it. We found no evidence that AIZ removal generated thermophilic movement (Fig. 3B). Laser ablation of RIA has been reported to abolish thermotaxis at all temperatures (4). We used two strategies for RIA ablation: cell-specific expression of recCaspase and of KillerRed. We found that destroying RIA in developed worms using KillerRed had no effect on thermophilic or cryophilic movement. Killing RIA with recCaspase had no effect on positive thermotaxis, but may reduce negative thermotaxis above

the  $T_s$ . In any case, RIA is not required for worms to exhibit positive or negative thermotaxis in our experimental setup (Fig. 3B).

Ablation of the AWC olfactory neurons has been reported to mildly disrupt negative thermotaxis down gradients toward the  $T_s$  (8). Because our setup supports both positive and negative thermotaxis, we examined AWC using both laser ablation and cell-specific expression of recCaspase. We found no significant disruption in either positive or negative thermotaxis after AWC removal (Fig. 3B).

**AFD Drives Thermotactic Behavior in Both Thermophilic and Cryophilic Animals.** Our results indicate that AFD regulates both positive and negative thermotaxis toward the  $T_s$ . We asked whether AFD also drives these behaviors in worms that aberrantly display positive thermotaxis by moving toward warmer temperatures even when above  $T_s$  (i.e., a thermophilic phenotype) or negative thermotaxis by moving toward colder temperatures even when below  $T_s$  (i.e., a cryophilic phenotype).

We performed a forward genetic screen to identify mutants that exhibited a strong thermophilic phenotype and isolated *pg5*, which robustly migrated up steep thermal gradients following cultivation at 15 °C and 25 °C (Fig. 3C). Three-factor and snip-SNP mapping placed the *pg5* mutation on the right side of chromosome V near the position of *pkc-1*. *pkc-1* (also known as *ttx-4*) has previously been implicated in thermotaxis (7). Complementation with a putative null allele, *njl*, revealed that *pg5* was an allele of *pkc-1*, as *pg5/njl* heterozygotes exhibited behavior that was indistinguishable from that of either mutant alone. Sequencing the *pkc-1* gene in *pg5* worms revealed a single nucleic acid substitution in the fifth exon, introducing a premature stop codon and indicating that *pg5* is likely to be a null allele of *pkc-1*. No other thermophilic mutants were isolated in the screen.

It has been shown that AFD-specific expression of wild-type *pkc-1* rescues its thermotaxis defect, suggesting that PKC signaling in AFD contributes to the display of negative vs. positive thermotaxis (7). To determine whether AFD output is needed to drive thermophilic movement in *pkc-1* mutants, we used a transgenic line that expressed recCaspase in AFD in a *pkc-1(pg5)* mutant background. Indeed, AFD ablation abolished thermotaxis both above and below the  $T_s$  (Fig. 3C).

Next, we asked whether AFD was required to produce negative thermotaxis in worms lacking the AIY interneuron, resulting either from mutation in *ttx-3(ks5)* or from genetic ablation of

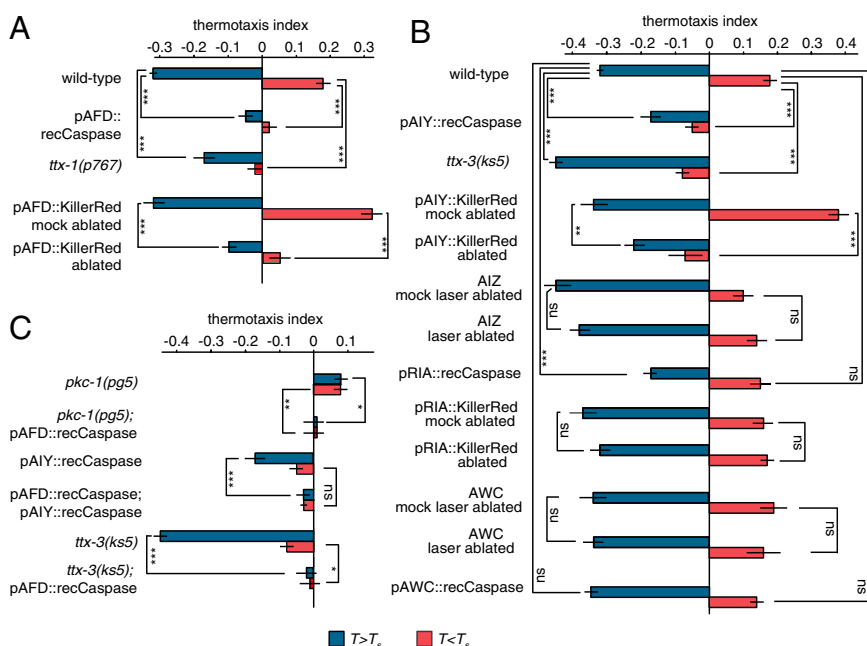


**Fig. 3.** Neuronal determinants of thermotaxis. (A) Analysis of AFD contributions to negative thermotaxis when  $T > T_s$  and to positive thermotaxis when  $T < T_s$ . (B) Analysis of other neurons in the proposed circuit for thermotaxis. (C) Analysis of AFD in mutant backgrounds that always crawl up or down temperature gradients. The thermotactic index—the ratio between mean velocity in the gradient direction and mean crawling speed (mean  $\pm$  1 SEM)—is calculated over the trajectories of individual worms when started at 20 °C and grown at 25 °C (red,  $T < T_s$ ) or when started at 20 °C and grown at 15 °C ( $T > T_s$ ). Salient comparisons between worms with intact neurons or disrupted neurons are shown. \* $P < 0.05$ ; \*\* $P < 0.005$ ; \*\*\* $P < 0.0005$  by Student *t* test. A total of 40–309 worms were used to calculate each index.



peptidergic signals (35, 36). One possibility is that AIY acts as a switch, shifting AFD output from driving negative thermotaxis to positive thermotaxis below the setpoint. The function of *pkc-1* acting in AFD may also contribute to the switching mechanism, helping to shift AFD output from driving positive thermotaxis to negative thermotaxis above the setpoint (Fig. 4C). Although AIY is the dominant postsynaptic partner of AFD, it is not needed to carry out the sensorimotor transformations that transform AFD activity into negative thermotaxis. The AWC olfactory neuron and the AIZ interneuron have been proposed to play roles in negative thermotaxis (4, 8, 27); we find that neither AWC nor AIZ is required for either positive or negative thermotaxis. RIA has been proposed to be required for both positive and negative thermotaxis (4). RIA has recently been found to represent a corollary discharge signal that conveys head movement to the upstream circuit (37). We do not believe that RIA plays an essential role in the thermotaxis behavior probed in our assays.

In summary, different modes of thermotaxis are driven by the AFD thermosensory neurons via different sensorimotor strategies. AFD intracellular signaling is sophisticated, involving a complex cGMP-dependent thermotransduction cascade and multiple forms of synaptic output including glutamatergic signaling, peptidergic signaling, and gap junctions (35, 36, 38, 39). The richness of AFD signal processing and synaptic output is likely to underlie its capacity to effect the appropriate mode of thermotactic behavior in different temperature regimes via downstream circuits that flexibly map AFD activity patterns to movement patterns.

- de Bono M, Maricq AV (2005) Neuronal substrates of complex behaviors in *C. elegans*. *Annu Rev Neurosci* 28:451–501.
- Hedgecock EM, Russell RL (1975) Normal and mutant thermotaxis in the nematode *Caenorhabditis elegans*. *Proc Natl Acad Sci USA* 72(10):4061–4065.
- Biron D, et al. (2006) A diacylglycerol kinase modulates long-term thermotactic behavioral plasticity in *C. elegans*. *Nat Neurosci* 9(12):1499–1505.
- Mori I, Ohshima Y (1995) Neural regulation of thermotaxis in *Caenorhabditis elegans*. *Nature* 376(6538):344–348.
- Chi CA, et al. (2007) Temperature and food mediate long-term thermotactic behavioral plasticity by association-independent mechanisms in *C. elegans*. *J Exp Biol* 210(Pt 22):4043–4052.
- Kimata T, Sasakura H, Ohnishi N, Nishio N, Mori I (2012) Thermotaxis of *C. elegans* as a model for temperature perception, neural information processing and neural plasticity. *Worm* 1(1):31–41.
- Okochi Y, Kimura KD, Ohta A, Mori I (2005) Diverse regulation of sensory signaling by *C. elegans* nPKC-epsilon/eta TTX-4. *EMBO J* 24(12):2127–2137.
- Biron D, Wasserman S, Thomas JH, Samuel ADT, Sengupta P (2008) An olfactory neuron responds stochastically to temperature and modulates *Caenorhabditis elegans* thermotactic behavior. *Proc Natl Acad Sci USA* 105(31):11002–11007.
- Swierczek NA, Giles AC, Rankin CH, Kerr RA (2011) High-throughput behavioral analysis in *C. elegans*. *Nat Methods* 8(7):592–598.
- Stephens GJ, Johnson-Kerner B, Bialek W, Ryu WS (2008) Dimensionality and dynamics in the behavior of *C. elegans*. *PLoS Comput Biol* 4(4):e1000028.
- Albrecht DR, Bargmann CI (2011) High-content behavioral analysis of *Caenorhabditis elegans* in precise spatiotemporal chemical environments. *Nat Methods* 8(7):599–605.
- Clark DA, Gabel CV, Lee TM, Samuel ADT (2007) Short-term adaptation and temporal processing in the cryophilic response of *Caenorhabditis elegans*. *J Neurophysiol* 97(3):1903–1910.
- Ryu WS, Samuel ADT (2002) Thermotaxis in *Caenorhabditis elegans* analyzed by measuring responses to defined Thermal stimuli. *J Neurosci* 22(13):5727–5733.
- Luo L, Clark DA, Biron D, Mahadevan L, Samuel ADT (2006) Sensorimotor control during isothermal tracking in *Caenorhabditis elegans*. *J Exp Biol* 209(Pt 23):4652–4662.
- Pierce-Shimomura JT, Morse TM, Lockery SR (1999) The fundamental role of pirouettes in *Caenorhabditis elegans* chemotaxis. *J Neurosci* 19(21):9557–9569.
- Berg HC, Brown DA (1972) Chemotaxis in *Escherichia coli* analysed by three-dimensional tracking. *Nature* 239(5374):500–504.
- Ramot D, MacLinnis BL, Lee H-C, Goodman MB (2008) Thermotaxis is a robust mechanism for thermoregulation in *Caenorhabditis elegans* nematodes. *J Neurosci* 28(47):12546–12557.
- Chelur DS, Chalfie M (2007) Targeted cell killing by reconstituted caspases. *Proc Natl Acad Sci USA* 104(7):2283–2288.
- Williams DC, et al. (2013) Rapid and permanent neuronal inactivation in vivo via subcellular generation of reactive oxygen with the use of KillerRed. *Cell Rep* 5(2):553–563.
- Bulina ME, et al. (2006) A genetically encoded photosensitizer. *Nat Biotechnol* 24(1):95–99.
- Iino Y, Yoshida K (2009) Parallel use of two behavioral mechanisms for chemotaxis in *Caenorhabditis elegans*. *J Neurosci* 29(17):5370–5380.

## Materials and Methods

**Strains, Cultivation, and Ablation Methods.** *C. elegans* were grown on bacterial lawns of the *Escherichia coli* strain OP50 overnight at 15 °C or 25 °C using standard methods (40). Strains used and the procedure for isolating the allele *pkc-1(pg5)* are described in *SI Materials and Methods*. Laser ablation, KillerRed-mediated ablation, and Caspase-mediated ablation were performed using previously described methods, described in detail in *SI Materials and Methods* (18, 19, 41).

**Behavioral Analysis.** High-throughput behavioral analysis using a large-format thermotaxis assay was devised by adapting previously described methods used for analyzing the navigational movements of *C. elegans* or *Drosophila* larva (12, 42). The high-resolution behavioral assay was generated by using a smaller version of the high-throughput behavioral assay mounted on a compound microscope. Descriptions of the apparatus and software are available in *SI Materials and Methods*.

**Calcium Imaging.** Calcium imaging followed previously described protocols for measuring the activity of the AFD neurons (31). Custom hardware for temperature control and spinning disk confocal microscopy that was used in this study is described in *SI Materials and Methods*. Data analysis was performed using MATLAB (Mathworks).

**ACKNOWLEDGMENTS.** This work was supported by National Science Foundation (NSF) Grant PHY-0957185 and National Institutes of Health (NIH) Grant 8DP1GM105383-05 (to A.D.T.S.), NSF Grant IOS0725079 and NIH Grant R21 NS061147 (to M.B.G.), a Human Frontier Science Program fellowship (to B.L.M.), NIH Grant 1P01GM103770 (to A.D.T.S. and Y.Z.), National Nature Science Foundation of China Grant 11304153 (to L.L.), and NIH Grant R01NS076558 (to D.A.C.-R.).

- Luo L, et al. (2010) Navigational decision making in *Drosophila* thermotaxis. *J Neurosci* 30(12):4261–4272.
- McCormick KE, Gaertner BE, Sottile M, Phillips PC, Lockery SR (2011) Microfluidic devices for analysis of spatial orientation behaviors in semi-restrained *Caenorhabditis elegans*. *PLoS ONE* 6(10):e25710.
- Chung SH, Clark DA, Gabel CV, Mazur E, Samuel ADT (2006) The role of the AFD neuron in *C. elegans* thermotaxis analyzed using femtosecond laser ablation. *BMC Neurosci* 7:30.
- Teh C, et al. (2010) Optogenetic in vivo cell manipulation in KillerRed-expressing zebrafish transgenics. *BMC Dev Biol* 10:110.
- Satterlee JS, et al. (2001) Specification of thermosensory neuron fate in *C. elegans* requires *ttx-1*, a homolog of *otd/Otx*. *Neuron* 31(6):943–956.
- Kuhara A, et al. (2008) Temperature sensing by an olfactory neuron in a circuit controlling behavior of *C. elegans*. *Science* 320(5877):803–807.
- Mori I, Sasakura H, Kuhara A (2007) Worm thermotaxis: A model system for analyzing thermosensation and neural plasticity. *Curr Opin Neurobiol* 17(6):712–719.
- Ramot D, MacLinnis BL, Goodman MB (2008) Bidirectional temperature-sensing by a single thermosensory neuron in *C. elegans*. *Nat Neurosci* 11(8):908–915.
- Kimura KD, Miyawaki A, Matsumoto K, Mori I (2004) The *C. elegans* thermosensory neuron AFD responds to warming. *Curr Biol* 14(14):1291–1295.
- Clark DA, Biron D, Sengupta P, Samuel ADT (2006) The AFD sensory neurons encode multiple functions underlying thermotactic behavior in *Caenorhabditis elegans*. *J Neurosci* 26(28):7444–7451.
- Clark DA, Gabel CV, Gabel H, Samuel ADT (2007) Temporal activity patterns in thermosensory neurons of freely moving *Caenorhabditis elegans* encode spatial thermal gradients. *J Neurosci* 27(23):6083–6090.
- Chen T-W, et al. (2013) Ultrasensitive fluorescent proteins for imaging neuronal activity. *Nature* 499(7458):295–300.
- White JG, Southgate E, Thomson JN, Brenner S (1986) The structure of the nervous system of the nematode *Caenorhabditis elegans*. *Philos Trans R Soc Lond B Biol Sci* 314(1165):1–340.
- Ohnishi N, Kuhara A, Nakamura F, Okochi Y, Mori I (2011) Bidirectional regulation of thermotaxis by glutamate transmissions in *Caenorhabditis elegans*. *EMBO J* 30(7):1376–1388.
- Narayan A, Laurent G, Sternberg PW (2011) Transfer characteristics of a thermosensory synapse in *Caenorhabditis elegans*. *Proc Natl Acad Sci USA* 108(23):9667–9672.
- Hendricks M, Ha H, Maffey N, Zhang Y (2012) Compartmentalized calcium dynamics in a *C. elegans* interneuron encode head movement. *Nature* 487(7405):99–103.
- Wang D, O'Halloran D, Goodman MB (2013) GCY-8, PDE-2, and NCS-1 are critical elements of the cGMP-dependent thermotransduction cascade in the AFD neurons responsible for *C. elegans* thermotaxis. *J Gen Physiol* 142(4):437–449.
- Chuang C-F, Vanhoven MK, Fetter RD, Verselis VK, Bargmann CI (2007) An innexin-dependent cell network establishes left-right neuronal asymmetry in *C. elegans*. *Cell* 129(4):787–799.
- Brenner S (1974) The genetics of *Caenorhabditis elegans*. *Genetics* 77(1):71–94.
- Fang-Yen C, Gabel CV, Samuel ADT, Bargmann CI, Avery L (2012) Laser microsurgery in *Caenorhabditis elegans*. *Methods Cell Biol* 107:177–206.
- Gershow M, et al. (2012) Controlling airborne cues to study small animal navigation. *Nat Methods* 9(3):290–296.